



# Incorporating fish orientation into target strength-total length equations: Horizontal-Aspect target-Strength equations for gizzard shad *Dorosoma cepedianum*

Garrett R. Johnson<sup>a,b,\*</sup>, Daniel E. Shoup<sup>a</sup>, Kevin M. Boswell<sup>c</sup>

<sup>a</sup> Oklahoma State University, Department of Natural Resource Ecology & Management, 008c Agricultural Hall, Stillwater, OK, 74078, USA

<sup>b</sup> Oklahoma Cooperative Fish and Wildlife Research Unit, 007 Agricultural Hall, Oklahoma State University, Stillwater, OK, 74078, USA

<sup>c</sup> Florida International University, Marine Sciences Program, Department of Biological Sciences, 3000 NE 151st Street North Miami, FL, 33181, USA

## ARTICLE INFO

Handled by George A. Rose

### Keywords:

Hydroacoustic  
Horizontal-aspect  
Target strength  
Gizzard shad

## ABSTRACT

Horizontally-oriented echosounders have become more common for sampling pelagic prey species in shallow waterbodies (e.g. < 20 m) or nearshore portions of deeper water bodies, where vertical beaming can be ineffective. To properly sample fishes with horizontally-oriented echosounders, a target-strength ( $TS$ ; dB re  $1 \text{ m}^2$ )-to-total-length ( $TL$ ; mm) relationship must be developed to acquire reliable density data. However, when sampling with horizontal beaming, measured  $TS$  can vary greatly according to fish orientation (lateral versus head-on). Currently, a  $TS$ - $TL$  equation that is based on  $TS$  data from individual fish measured at all orientations is used to convert between  $TL$  and measured  $TS$ . However, an orientation-based equation (equation that incorporates target orientation information when converting  $TS$  to  $TL$ ) could increase the accuracy of size estimates from direct  $TS$  measurements. Target strength measurements were collected from euthanized Gizzard Shad *Dorosoma cepedianum*, in a tank, at orientations from 0 to 180° (0° and 180° being perpendicular to acoustic beam and 90° parallel with head facing the transducer) in 5° increments. We derived orientation-based and non-orientation-based  $TS$ - $TL$  equations for Gizzard Shad. Eight orientation-based equations were compared with a catenary (U-Shape) function best representing the change in  $TS$  for different fish orientations (conditional  $R^2 = 0.71$  and marginal  $R^2 = 0.67$ ). Our orientation-based equation can be used to acquire more accurate Gizzard Shad biomass estimates when orientation information is available. We found significant errors occur when using an average-orientation  $TS$ - $TL$  equation when fish do not have random orientation, so orientation-based equations should be used when possible. We also compared density estimates from previously published, non-orientation-based  $TS_{\text{Mean}}$  equations ( $TS$ - $TL$  equation derived from mean  $TS$  of all target orientations) to determine if equation choice significantly affected density estimates from fish aggregations. Equation choice had a significant effect on the resulting density estimates from individual schools ( $P < 0.01$ ), indicating species-specific equations provide greater accuracy.

## 1. Introduction

The use of horizontally-oriented single-beam echosounders for sampling pelagic prey species has recently become more common in shallow (e.g., < 20 m) waterbodies and nearshore areas where vertical beaming can be ineffective (Balk et al., 2017; Lian et al., 2017). Vertically-oriented hydroacoustic techniques are ineffective in shallow water because they do not sample near-surface or near-substrate areas effectively, resulting in a small volume of water sampled (Simmonds and MacLennan, 2005; Thorne, 1998). Hypoxic regions caused by thermal stratification can further reduce the proportion of the water

column available to fish as habitat, further limiting the efficiency of vertically-oriented echosounders (Roberts et al., 2009). The net result is reduced ability to collect meaningful vertically-oriented hydroacoustic data in shallow systems. However, horizontally-oriented echosounders show promise as a sampling tool for pelagic prey species in shallow waterbodies and nearshore areas of deeper waterbodies because they can efficiently collect large amounts of data and effectively sample near-surface fish (Djemali et al., 2017; Knudsen and Sægrov, 2002; Kubečka and Wittingerova, 1998; Thorne, 1998; Yule, 2000). Although horizontally oriented echosounders have limitations as well, including near surface reverberation (Balk et al., 2017; Trevorrow, 1998; Urlick

\* Corresponding author.

E-mail addresses: [garrerj@okstate.edu](mailto:garrerj@okstate.edu) (G.R. Johnson), [daniel.shoup@okstate.edu](mailto:daniel.shoup@okstate.edu) (D.E. Shoup), [kevin.boswell@fiu.edu](mailto:kevin.boswell@fiu.edu) (K.M. Boswell).

and Hoover, 1956), range limitations (Pedersen and Trevorrow, 1999), noise (Balk et al., 2017; Boswell et al., 2007; Pollom and Rose, 2015) and fish behavior (Draštík and Kubečka, 2005; Vabø et al., 2002), a horizontal approach addresses many of the limitations of vertically oriented echosounders.

Target strength (*TS*; ratio of the intensity of the reflected wave at a distance of 1 m to the incident sound wave; dB re 1 m<sup>2</sup>) describes the acoustic reflectivity of an ensonified target (Simmonds and MacLennan, 2005). Target strength measurements can be obtained from unconstrained wild fishes (in situ; Fleischer et al., 1997; Pedersen et al., 2009; Warner et al., 2002), constrained or sedated fishes (ex situ; Nielsen and Lundgren, 1999; Rodríguez-Sánchez et al., 2015; Thomas et al., 2002) or by modelling fish and swim bladder size and shape (Gorska and Ona, 2003; McClatchie et al., 1998; Peña and Foote, 2008). Because *TS* is a proxy for fish size, *TS* data are imperative when estimating biomass from hydroacoustic data (MacLennan and Simmonds, 2013; Simmonds and MacLennan, 2005). When *in-situ* *TS* measurements are unavailable, equations converting fish size to *TS* allow length data from concurrently sample fish to be converted to *TS* for use in hydroacoustic analyses (Boswell et al., 2008; Gastauer et al., 2017; Kubečka et al., 2009; Scoulding et al., 2017).

Given that *TS* is a function of the cross-sectional area of the ensonified target, changes in animal orientation can result large variation in measured *TS*, particularly when ensonified in the horizontal plane (Boswell and Wilson, 2008; Rodríguez-Sánchez et al., 2015). Fish air bladders, when present, reflect 90–95% of the total energy reflected by an individual (Foote, 1980). Generally, air bladders have an elongate shape that has a smaller ensonified cross-sectional area when the fish faces the transducer than when it is oriented perpendicular to the main axis (Foote, 1980; Kubečka and Duncan, 1998a). Fish orientation is less problematic with vertical beaming because the dorsal surfaces of fish are almost always ensonified (hence the long axis of the air bladder), unless data are collected during periods of vertical migration (Harden-Jones et al. 1981). In current horizontal hydroacoustic applications, an average target strength- total length (*TS-TL*; regression describing the mean *TS*-mean length relationship) or target strength-weight (*TS-W*; regression describing mean *TS*-mean weight relationship) equation is often implemented, where *TS* is averaged from measurements at all fish lateral orientations (Boswell et al., 2008; Frouzova et al., 2005). As long as fish orientation is random, a mean *TS-TL* equation is acceptable and produces minimal bias because *TS* is measured for targets at all orientations and thus an average *TS* accounts for orientation (Boswell et al., 2008; Lilja et al., 2000). However, fish may not be randomly oriented due to boat avoidance, fish facing into current, migratory movements or schooling patterns (Draštík and Kubečka, 2005; Lilja, 2004; Weihs, 1973). Therefore, incorporating fish orientation into *TS-TL* equations could increase accuracy and precision of horizontal hydroacoustic biomass estimates in cases where the assumption of random orientation is not met. Kubečka (1994) proposed a model to describe change in *TS* with orientation for Brown Trout *Salmo trutta*, Roach *Rutilus rutilus* and Rudd *Scardinius erythrophthalmus*, but the equation only considered a single curve shape and did not account for fish length (Kubečka, 1994). Lilja et al. (2000) added fish length to the aspect equation proposed by Kubečka (1994) and derived coefficients for Atlantic Salmon (*Salmo salar*), Pike (*Esox Lucius*), Brown Trout and Whitefish *Coregonus lavaretus*. Because Kubečka (1994)'s equations were not fit for all species, more information is needed before applying Kubečka (1994)'s equation to species beyond the four species tested by Lilja et al. (2000).

Target orientation can be measured in multiple ways. Recent approaches infer fish orientation from the trajectory of tracked targets across successive pings (Rodríguez-Sánchez et al., 2015) and improvements in broadband SONAR technology have resulted in an ability to infer target orientation through increased range resolution and improved interpretation of scattering features of individual targets (Ito et al., 2015; Lavery et al., 2017; Lee and Stanton, 2016; Lundgren and

Nielsen, 2008; Stanton et al., 2003). There is potential to further refine horizontal data by combining split-beam transducers with multi-beam imaging systems (i.e. ARIS® or DIDSON®) that can measure fish orientation directly. With these methods to detect fish orientation, *TS* equations can be developed that more accurately identify fish size from *TS* measured at any angle.

Gizzard Shad (*Dorosoma cepedianum*) is an important pelagic prey species in shallow reservoirs and often the most abundant prey species in southern and mid latitudes in the United States. (Carline et al., 1984; Johnson et al., 1988; Miranda, 1983). Because Gizzard Shad have high densities, they are often a large portion of piscivore diets (Michaletz, 1997; Storck, 1986). Gizzard Shad populations can frequently be limiting (Evans et al., 2014) and therefore have a large impact on growth and survival of piscivorous species (Michaletz, 1997, 1998; Schramm et al., 1999; Storck, 1986). Therefore, Gizzard Shad can have a large impact on populations of piscivorous fishes, making accurate density and size structure data for Gizzard Shad important to fisheries managers managing piscivorous species.

Currently, gill nets are used to collect Gizzard Shad abundance and size structure data for use in fisheries management, a sampling method that is time and labor intensive, as well as imprecise (Van Den Avyle et al., 1995a; Wilde, 1995). Horizontally-oriented echosounders may provide more reliable data than current sampling methods for pelagic fish populations (such as Gizzard Shad) in shallow systems (Johnson et al., 2019; Van Den Avyle et al., 1995a, b), but only if fish sizes can be accurately estimated from *TS* measurements or *TS* estimated from concurrent catch data. Development of species-specific *TS-TL* and *TS-W* equations could increase accuracy of biomass estimates, but no horizontal *TS-TL* or *TS-W* equation exists for Gizzard Shad, and the equations that do exist for other species have used fairly simplified approaches that have not thoroughly evaluated the quality of the fit to the data (Godlewska et al., 2012; Kubečka, 1994; Pedersen et al., 2009). Incorporating target orientation may further increase accuracy of hydroacoustic estimates when orientation information is available (Boswell et al., 2009; Kubečka, 1994; Lilja et al., 2000). Our goal is to develop *TS-TL* and *TS-W* equations for Gizzard Shad and then to determine if equation choice (our equation versus previously reported equations derived with other species) significantly affected density estimates from echo integration of fish aggregations. Additionally, we propose orientation-based equations that predict *TL* from *TS* and orientation data and compare them to equations by (Kubečka, 1994) to determine which equation best predicts Gizzard Shad size. This information can be used to better inform Gizzard Shad horizontally-oriented echosounder data analyses.

## 2. Methods

### 2.1. Tethered fish experiments

Target strength measurements were collected July to September 2017 in a 5.5 m diameter round tank, filled to 1 m depth, inside the Fisheries and Aquatic Ecology Wet Laboratory (FAEWL) at Oklahoma State University. Forty-seven Gizzard Shad were collected from nearby Lake Carl Blackwell, Payne County, Oklahoma (OK) using boat electrofishing and were transported live in an aerated live tank to the FAEWL. Fish were transferred to an aerated holding tank with a mean water temperature of 22 °C (standard deviation [s.d.] = 1.65, range 20–25 °C) and allowed to acclimate for at least 24 h before experimentation.

Individual Gizzard Shad (60–321 mm *TL*) were euthanized using 150 mg/L Aqui-S 20E and tethered upright, one at a time, to a rotating carousel at a depth of 0.5 m using four strands of 2.7 kg monofilament fishing line (Fig. 1). Wet weights (*W*; g) and total lengths (*TL*; mm) were recorded for individuals prior to tethering. Below the carousel, a horizontal monofilament line was stretched tight along the tank bottom between two cinder blocks that were outside the acoustic beam. Two

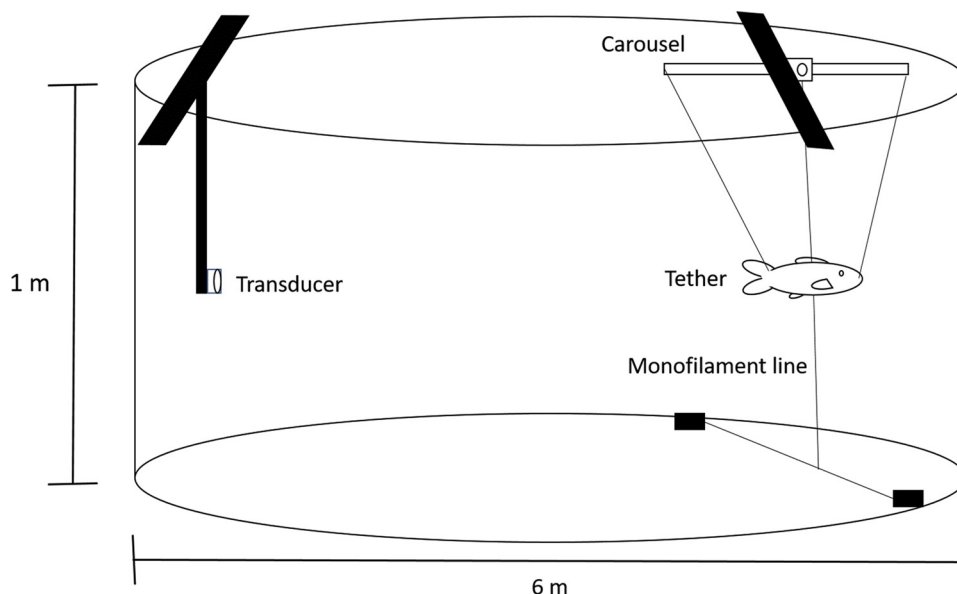


Fig. 1. Diagram depicting setup of transducer and tethered fish within a tank for *ex situ* hydroacoustic target strength measurements of Gizzard Shad.

vertical pieces of monofilament line were used to suspend fish between the carousel and the horizontal line at the tank bottom. One piece of monofilament was threaded through flesh at the dorsal surface of the fish and attached to the carousel, the other was threaded through the ventral surface of the fish and attached to the horizontal line at the tank bottom. Two separate monofilament lines were then threaded through flesh at the mouth and caudal peduncle and connected to the carousel to maintain fish at the desired orientation. All monofilament lines were attached to the fish in a way that did not puncture the air bladder (Fig. 1). The rotating carousel was built using a 72-tooth rotating sprocket, allowing for rotation in 5° increments.

Hydroacoustic data were collected with a Simrad® EK60 split-beam echosounder (See Table 1 for parameter settings) operating at 120 kHz with a 7° beam angle. The transducer was mounted along the tank wall facing horizontally across the tank at a depth of 0.5 m (Fig. 1). This put the tethered Gizzard Shad approximately 4 m (beam diameter 0.5 m) away from the transducer, which was greater than the transducer nearfield (0.86 m) plus the nearfield of the largest ensouffled fish

(321 mm; Rodríguez-Sánchez et al., 2016) and ensured the entire fish was within the beam. A pulse duration of 0.256 ms (pulse length 0.37 m) was chosen based on the Great Lakes freshwater sampling protocol (Parker-Stetter et al., 2009). Tethered fish were positioned at least 1 m from the back wall centered within the transducer's acoustic beam before recording. The tank wall, which was more than twice the pulse length from the fish, had a much stronger *TS* than tethered fish ( $\geq -10$  dB re  $1 \text{ m}^2$ ), allowing for clear separation of the target from the back wall. The echosounder was calibrated using a 38.1-mm diameter tungsten-carbide calibration sphere with ~6% cobalt binder following standard sphere methodology (Foote, 1987a). Data were collected at 4 Hz for at least 1 min at each orientation from 0 to 180° in 5° increments (0 and 180 being perpendicular to acoustic beam and 90° being parallel with head facing the transducer) resulting in 36 positions and at least 8640 *TS* measurements for each fish. A minimum threshold of -70 dB re  $1 \text{ m}^2$  was used, which was more than adequate to eliminate background noise (-85 dB re  $1 \text{ m}^2$ ) and echoes from the monofilament line. Measured *TS* was back-transformed to backscattering cross-section ( $\sigma_{bs}$ ,  $\text{m}^2$ ) before all computations ( $\sigma_{bs} = 10^{(TS/10)}$ ).

We derived orientation- and non-orientation-based *TS*-*TL* equations and a *TS*-*W* equation for Gizzard Shad using the data recorded from tethered fish. Non-orientation-based *TS*-*TL* equations were of the traditional form ( $a * \log_{10} TL + b$ ) and a second variant of the equation with the slope ( $a$ ) fixed at 20, as proposed by Foote (1987b). We fit equations to the mean ( $TS_{\text{Mean}}$ ), maximum ( $TS_{\text{Lateral}}$ ) and minimum ( $TS_{\text{Head/Tail}}$ ) of all *TS* measurements for individual fish as suggested by Frouzova et al. (2005). We tested for significant differences ( $\alpha = 0.05$ ) between slopes ( $a$ ) and intercepts ( $b$ ) of the standard and Foote (1987b)-variant *TS*-*TL* relationships for the three pairs of equations (i.e., equations derived from mean, maximum and minimum *TS*) using a t-test. Based on the observation that *TS* was strongest at 0° and 180° and weakest at 90° (Fig. 2), we identified five different functions that appropriately modelled orientation-specific *TS*-*TL* relationships (Table 2). Proposed orientation-based functions include two trigonometric functions,  $\text{Trig}_{\text{sin}}$  which uses only a sin term and  $\text{Trig}_{\text{both}}$  using both a sin and cosine function, a second degree polynomial function ( $\text{Poly}_2$ ), a catenary function (Catenary) which describes the hanging of a chain and an absolute value function (ABV; Table 2). We compared these five functions and three additional equations proposed by Kubečka (1994), as modified by Lilja et al. (2000) to include *TL*, and the non-orientation-based equations that were derived from mean *TS* (Table 2).

We fit each equation to *TS* data from tethered fish using maximum

Table 1

Echosounder, transducer and analysis thresholds used in laboratory target-strength experiments for Gizzard Shad and during a drift survey in Lake Carl Blackwell, Stillwater, Oklahoma.

System parameters	Laboratory	Field
<b>SIMRAD EK60 split-beam echosounder</b>		
Transmitted Power (W)	200	200
Operating Frequency (kHz)	120	120
Pulse Duration (ms)	0.256	0.256
Pulse rate (Hz)	4	10
<b>Transducer Parameters</b>		
Two way beam angle (dB re 1 sr)	-20.7	-20.7
Beam width (degrees)	7	7
Nearfield range (m)	0.86	0.86
<b>Echoview Analysis Threshold</b>		
<i>TS</i> (dB re $1 \text{ m}^2$ )	-70	-65
Single target detector settings		
Pulse length determination level	6	
Minimum normalized pulse length	0.5	
maximum normalized pulse length	1.8	
Maximum beam compensation (dB re $1 \text{ m}^2$ )	11	
Maximum standard deviation of		
Minor axis angle (degrees)	3	
major-axis angles (degrees)	3	

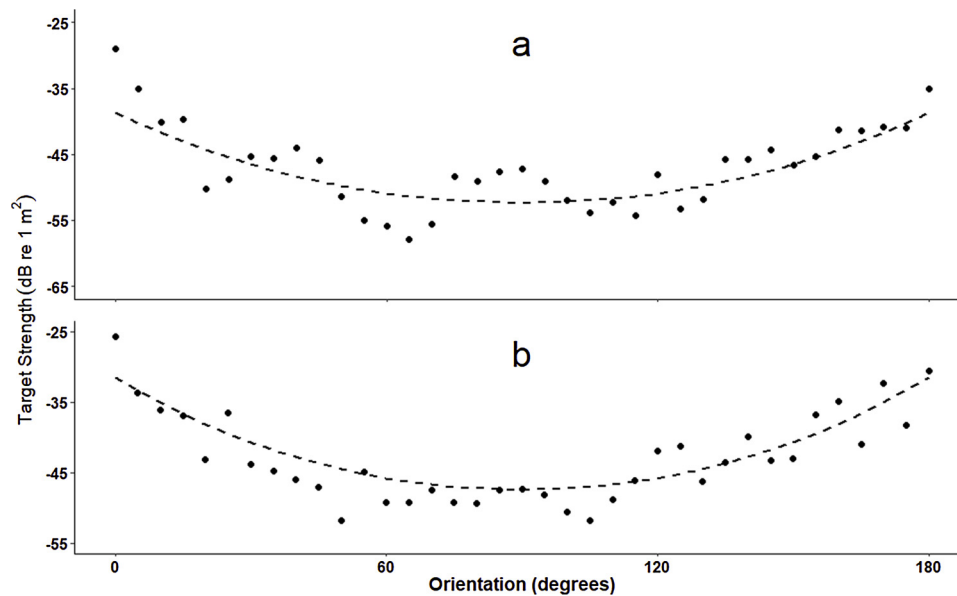


Fig. 2. Example of target strengths for 142-mm (a) and 267-mm (b) Gizzard Shad at orientations ranging from 0 to 180 degrees (0 and 180 being lateral and 90 being head-on perspective) in 5° increments from *ex situ* experiments. Dashed line represents predicted TS from catenary function described in methods and results.

likelihood estimation and assessed the most parsimonious equation using AIC. Target strength responses from all fish were fit simultaneously using a linear mixed effects model with fish size ( $\log_{10}(TL)$ ) and orientation (radians) as fixed factors and individual fish as a random factor (to account for repeated measurements on individuals) using the nlme package in R (Pinheiro et al., 2017). We tested all interaction terms iteratively and removed non-significant interaction terms from each model separately. Conditional and marginal  $R^2$  values were then calculated and residual plots were viewed to evaluate model fit. The  $TL$  estimates (i.e., compared with known fish size) from each of the above equations was then compared to determine the accuracy and uncertainty associated with the use of each equation.

2.2. Field test of TS-TL equation

To test the accuracy of our best orientation-based equation, we paired a Simrad® EK60 120 kHz echosounder (operating a 7° split-beam

transducer) with an ARIS® Explorer 1800 imaging SONAR operating at 1.8 MHz and recorded individual Gizzard Shad simultaneously in a net pen in the field (Lake Carl Blackwell, Stillwater, OK) to examine how well TS-derived fish size estimates matched fish size estimates derived from the imaging sonar. To ensure that only Gizzard Shad data were collected, fish were collected by boat-mounted electrofishing and placed within a nylon net pen (15-m long x 15-m wide x 4.5-m deep with 6.35-mm square mesh) located within the lake. Echosounder data were collected using settings specified in Table 1. Both systems were mounted in tandem on a bracket and lowered to a depth of 1 m within one side of the net pen. The sonars were aimed across the pen and angled 3.5° downward from horizontal to reduce surface noise. During data collection, the boat was pulled along one side of the net at a speed of 0.1 m/s. These data were collected at night when shad species are less aggregated, making it easier to measure isolated targets (Schael et al., 1995). Fish length and orientation for individual fish targets were estimated using the ARIS® imaging SONAR, capable of collecting high-

Table 2

Equations that were compared for estimating target strength using orientation and total length information where  $TS$  is predicted target strength ( $\text{dB re } 1 \text{ m}^2$ ),  $TL$  is total length (in mm),  $\sin$  is sine,  $\cos$  is cosine,  $\cosh$  is hyperbolic cosine, and  $\theta$  is orientation of the ensonified fish in radians where  $0^\circ$  (0 radians) and  $180^\circ$  ( $\pi$  radians) are perpendicular and  $90^\circ$  ( $\pi/2$  radians) is parallel to the transducer. Other symbols are constants fit by maximum likelihood. Proposed orientation-based functions include two trigonometric functions,  $\text{Trig}_{\sin}$  which uses only a sin term and  $\text{Trig}_{\text{both}}$  using both a sin and cos function, a second-degree polynomial function ( $\text{Poly}_2$ ), a catenary function (Catenary) which describes the hanging of a chain, an absolute value function (ABV) and three functions from Kubečka, 1994 (Kub,  $\text{Kub}_3$ ,  $\text{Kub}_5$ ). Two non-orientation equations include the standard  $TS_{\text{Mean}}$  equation with slope and intercept fitted (Non-orient) and the Foote, 1987b variant (Foote) with slope fitted at 20 using Gizzard Shad data.

Model Name	Equation
$\text{Trig}_{\sin}$	$= a * \sin \theta + b * \log_{10} TL + c * (\log_{10} TL * \sin \theta) + d$
$\text{Trig}_{\text{both}}$	$= (a * \cos \theta) + (b * \sin \theta) + c * \log_{10} TL + d * (\sin \theta) * \log_{10} TL + e$
$\text{Poly}_2$	$= a * ((\theta - 90^0)^2) + b * (\theta - 90^0) + c * \log_{10} TL + d * ((\theta - 90^0)^2 * \log_{10} TL) + e$
Catenary	$= \left( a * 1.57567 * \cosh \left( \frac{\theta - 90^0}{1.57567} \right) \right) + b * \log_{10} TL + c * \left( a * 1.57567 * \cosh \left( \frac{\theta - 90^0}{1.57567} \right) * \log_{10} TL \right) + d$
ABV	$= a *  (\theta - 90^0)  + b * \log_{10} TL + c * (\log_{10} TL *  (\theta - 90^0) ) + d$
Kub	$= a * \cos 2\theta + b * \log_{10} TL + c * (\cos 2\theta * \log_{10} TL) + d$
$\text{Kub}_3$	$= a * \cos^3 2\theta + b * \log_{10} TL + c * ((\cos^3 2\theta) * \log_{10} TL) + d$
$\text{Kub}_5$	$= a * \cos^5 2\theta + b * \log_{10} TL + c * ((\cos^5 2\theta) * \log_{10} TL) + d$
Non-orient	$= a * \log_{10} TL + b$
Foote	$= 20 * \log_{10} TL + b_{20}$

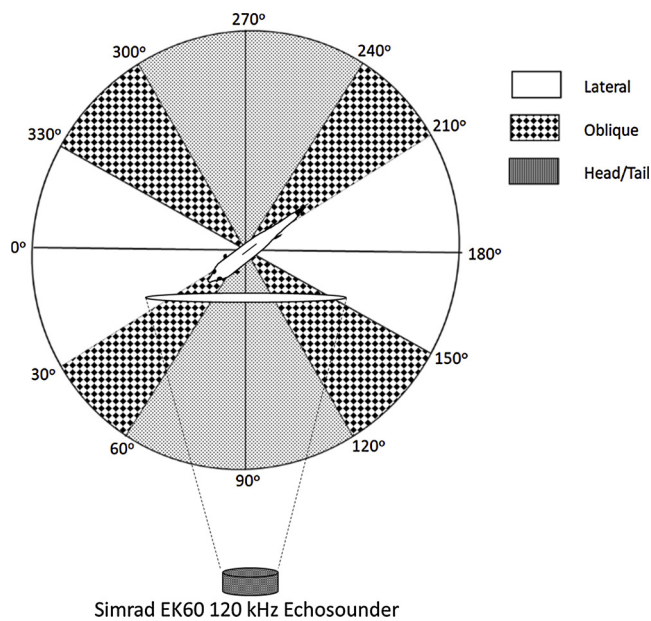


Fig. 3. Diagram of fish orientations within acoustic beam. Depicted fish is at an orientation of approximately 35° (oblique category).

resolution data (3-mm resolution; maximum range 15 m). During the analysis, both data from the echosounder and the imaging sonar were synchronized in Echoview® 8.1 to facilitate direct comparisons of sample data. We randomly selected 235 fish (60–267 mm TL) from the ARIS® data by selecting a random starting ping within a recording and selecting the first fish observed after this starting ping. Pings were not replaced so fish could not be measured twice. We manually measured the length and orientation of each selected fish from the ARIS® data, then recorded up to ten TS values from the corresponding fish track observed with the split-beam echosounder. Target strength values were converted to backscattering cross-section, averaged and back-transformed to derive a mean TS estimate. We converted the ARIS®-derived lengths to predicted TS's using the best performing orientation-based equation (hereafter called predicted TS). To consider the performance of the TS-TL equation at different fish orientations, orientations were categorized as lateral (perpendicular to transducer; 330° – 30° or 150° – 210°), oblique (30° – 60°, 120° – 150°, 210° – 240°, or 300° – 330°), or parallel (facing towards or away from transducer; 60° – 120° or 240° – 300°; Fig. 3) for the analysis. We then compared predicted TS (based on ARIS®-measured TL and orientation and our regression equation) with measured TS (from the split-beam echosounder) using an ANOVA with TS source (measured or predicted), length bin (25 mm groupings from 50 to 275 mm TL), and orientation group (lateral, oblique, or parallel) as fixed effects, trial (specific recording/date) as a random effect, and TS (measured or predicted depending on the TS source) as the response variable. This analysis was conducted in SAS (SAS Proc Glimmix; SAS Institute Inc, 2017) with a lognormal distribution to preserve scale

because the appropriate distribution (lognormal) was not available in program R.

### 2.3. Estimating uncertainty in biomass estimates caused by orientation changes

To estimate uncertainty in biomass estimates associated with incorrectly applied TS values (i.e., incorrect orientation assumptions), we used a similar approach to Boswell et al. (2009). Specifically, we used three hypothetical populations consisting of 1000 Gizzard Shad. The first population contained fish of identical length (150 mm). The second population had a uniform distribution of fish (100–200 mm) with a mean of 150 mm. The third population contained length distributions derived from a normal distributions of lengths from three age-classes: age-0 with a mean length of 100 mm (s.d. = 5; n = 750), age-1 with a mean length of 150 mm (s.d. = 7.5; n = 200), and age-2 with a mean length of 190 mm (s.d. = 10; n = 50). We then used simulations with these populations to quantify the effect of orientation errors on biomass calculated from TS-TL equations with incorrect orientations. We defined “true target strength” ( $TS_{true}$ ) for fish in the hypothetical populations as the target strength derived using fish length and our  $TS_{Lateral}$  equation (i.e., correct TS when fish is oriented laterally to transducer). We then used our orientation-based equation to determine what percentage of  $TS_{true}$  would be measured if the fish were at a defined orientation other than lateral to the transducer, which we defined as the  $TS_{apparent}$  (similar to  $TS_{ACT}$  in Boswell et al., 2009). We treated  $TS_{apparent}$  as if it was the TS measured in the field and estimated fish TL using the  $TS_{Lateral}$  equation. This produced an erroneous length (as a result of failing to meet the orientation assumption of the equation), which was then used with a length-mass conversion for Gizzard Shad (Jester and Jensen, 1972) to calculate the apparent total biomass of the fish aggregation at that fish orientation. This procedure was conducted for 19 different orientations from 0 to 90° in 5° increments (i.e., where 0° is the true lateral orientation and all other orientations represent differing degrees of orientation error up to 90°). All calculations were performed after converting TS to backscattering cross-section. True biomass was calculated using the defined length of the fish in the aggregation (i.e., Jester and Jensen 1972 length-mass conversion) and apparent biomass was calculated from TL estimated with known orientation errors (i.e., TL estimated from  $TS_{apparent}$  and the  $TS_{Lateral}$  equation). Proportional biomass was calculated to quantify the percent error caused by erroneous orientations and was calculated by dividing each apparent biomass by true biomass. We then compared true biomass and proportional biomass calculated from the 20 different simulated aggregation orientations to determine how biomass estimates differ depending on fish orientation.

### 2.4. Comparison of echo-integration results from different side-aspect TS-TL equations

To compare our non-orientation equations with other published horizontal-aspect equations (Table 3), we collected data from fish

Table 3  
Equations compared for accuracy when used in echo integrating analysis with individual schools of Gizzard Shad.

Name	Species	Equation	Source
<b>Lateral all aspect equations</b>			
John <sub>All</sub>	<i>Dorosoma cepedianum</i>	$23.02 * \log_{10}(TL_{mm}) - 93.53$	Current study
Frou <sub>pooled</sub>	<i>Salmo trutta</i> , <i>Perca fluviatilis</i> , <i>Abramis brama</i> , <i>Rutilus rutilus</i> , <i>Cyprinus carpio</i> , <i>Alburnus alburnus</i>	$24.26 * \log_{10}(TL_{mm}) - 100.68$	Frouzova et al. (2005)
BO <sub>pooled</sub>	<i>Brevoortia patronus</i> , <i>Anchoa mitchilli</i>	$14.5 * \log_{10}(TL_{cm}) - 60.8$	Boswell and Wilson (2008)
Kub <sub>All</sub>	<i>Rutilus rutilus</i> , <i>Salmo Trutta</i> , <i>Scardinius erythrophthalmus</i>	$34.1 * \log_{10}(TL_{mm}) - 114.3$	Kubečka (1994)
<b>Foote 1987 Variants</b>			
BO <sub>foote</sub>	<i>Brevoortia patronus</i> , <i>Anchoa mitchilli</i>	$20 * \log_{10}(TL_{cm}) - 65$	Boswell and Wilson (2008)
John <sub>foote</sub>	<i>Dorosoma cepedianum</i>	$20 * \log_{10}(TL_{mm}) - 86.42$	Current study

aggregations (aggregation size = 1–18 m<sup>2</sup>; multiple individual fish too densely aggregated to detect individual fish tracks with the echosounder) while drifting (100–500 m transects) in Lake Carl Blackwell, Stillwater, Oklahoma using both an ARIS® imaging SONAR operating at a frequency of 1.8 MHz (3 mm resolution) and a Simrad® 120 kHz split-beam echosounder with ping rate of 10 Hz (Table 1). Orientation-based equations were not tested because fish within aggregations in the reservoir were randomly oriented (based on imaging SONAR data), so orientation was not expected to strongly affect echo integration results in this case. Both sonars were mounted on an aluminum bracket that was angled downward 3.5° from horizontal and lowered to a depth of 1 m. Total-length data were collected from all fish in each aggregation using the ARIS®. Using these total length data, we calculated a mean TL for each of 23 schools observed. Mean TLs were then converted to a mean *TS* using each of six *TS*-TL equations (Table 3). We then echo-integrated each aggregation and scaled by the mean *TS* to acquire density estimates for each aggregation (Foote, 1987b; Foote et al., 1986; MacLennan and Simmonds, 2013; Scoulding et al., 2017). In addition to the two non-orientation based mean *TS*-TL equations (John<sub>All</sub> and John<sub>Foote</sub>) from the current study, we also tested Boswell and Wilson (2008) equations from pooled data for Gulf Menhaden *Brevoortia patronus* and Bay Anchovy (*Anchoa mitchilli*; Bos<sub>pooled</sub> and Bos<sub>Foote</sub>), Frouzova's (2005) European pooled freshwater fish equation (Fro<sub>U</sub><sub>pooled</sub>), and Kubečka's (1994) Brown Trout (*Salmo trutta*) equation (Kub<sub>All</sub>). Density estimates were calculated via echo integration for all 23 aggregations based on each of the mean *TS* estimates derived from the six mean *TS*-TL equations by scaling *S<sub>v</sub>* by the mean *TS* within the same volume (Simmonds and MacLennan, 2005). Echo-integrated aggregation densities from each of the six equations were then compared using ANOVA with *TS*-TL equation as a fixed factor and aggregation ID as a random factor using package lmerTest in Program R (Kuznetsova et al., 2017).

### 3. Results

#### 3.1. Tethered fish experiments

Despite having a relatively uniform distribution of fish lengths, mean *TS* of all fish at all measured orientations was -40.11 dB re 1 m<sup>2</sup> (SD = 7.4) with highest *TS* frequencies occurring from -45 to -50 dB re 1 m<sup>2</sup> (Fig. 4). Target strength distributions for fish of different sizes had substantial overlap when all orientations were measured, even for individuals of vastly different sizes (Fig. 4).

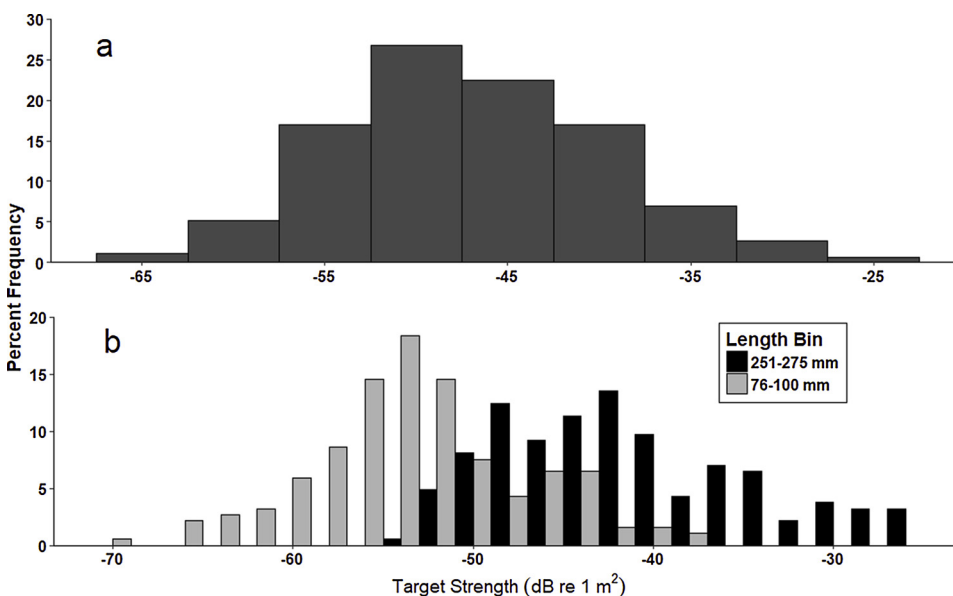


Fig. 4. Target-strength frequency for Gizzard Shad ( $n = 47,64\text{--}321$  mm,  $3\text{--}223.8$  g) at orientations from 0 to 180 degrees (0 and 180 being lateral and 90 being head-on perspective) measured *ex situ* tank trials (a) and distributions of *TS* measurements for Gizzard Shad in the 76–100 mm ( $n = 5$  fish, 185 measurements) and 251–275 mm ( $n = 5$  fish, 185 measurements) length bins at orientations from 0 to 180 degrees measured in *ex situ* tank trials illustrating overlap of measured target strength of large and small Gizzard Shad (b).

Regression equations for the  $TS_{\text{Lateral}}$ ,  $TS_{\text{head/tail}}$  and  $TS_{\text{Mean}}$  (both with fitted slopes and the Foote (1987b) variant with slope = 20) produced significant relationships (Fig. 5). For the  $TS_{\text{Mean}}$  equations (23.02), the fitted-slope equation had a significantly higher slope than the Foote (1987b) variant (20) equation ( $t = 2.32$ , d.f. = 91,  $P = 0.02$ ), whereas slopes of the  $TS_{\text{Lateral}}$  ( $t = 1.65$ , d.f. = 91,  $P = 0.10$ ) and  $TS_{\text{Head/Tail}}$  ( $t = 0.62$ , d.f. = 91,  $P = 0.53$ ) equations, 23.77 and 18.66 respectively, were not significantly different than the Foote (1987b) variants ( $\alpha = 20$  for each; Table 4). There were no significant differences between intercepts from the standard and Foote (1987b) variant equations for  $TS_{\text{Mean}}$  ( $t = 1.77$ , d.f. = 91,  $P = 0.08$ ),  $TS_{\text{Lateral}}$  ( $t = 0.81$ , d.f. = 91,  $P = 0.41$ ) or  $TS_{\text{Head/Tail}}$  ( $t = 0.33$ , d.f. = 91,  $P = 0.73$ ; Table 4). *TS*-W relationships from mean, maximum, and minimum *TS* data had  $R^2$  values of 0.85, 0.69, and 0.63 respectively (Table 4).

Measured *TS* of all fish increased as fish were rotated from head/tail perspective to lateral orientations (Fig. 2). The best orientation-based model was a catenary function with a significant interaction between the catenary term and  $\log_{10} TL$ , which fit as:

$$TS = \left( -4.57 * 1.58 * \cosh \left( \frac{\theta - 90^0}{1.58} \right) \right) + 2.68 * \log_{10} TL + 9.63 \\ * \left( 1.58 * \cosh \left( \frac{\theta - 90^0}{1.58} \right) * \log_{10} TL \right) - 83.57$$

(Table 5). The catenary model produced a U-shaped response for individual fish (Fig. 2) and formed a U-shape plane that curved upward when all fish sizes are considered (Fig. 6). All model parameters were significant and the conditional and marginal  $R^2$  values were 0.71 and 0.67, respectively.

#### 3.2. Field test of *TS*-TL equation

Target strengths predicted by the catenary model using measured lengths from the ARIS system were significantly greater than target strengths measured by the split-beam sonar at several orientation and length categories (Fig. 7). Predicted *TS* was significantly greater (3–4 dB re 1 m<sup>2</sup> different) than measured *TS* for fish between 151 and 225-mm *TL* ( $F_{16,410} = 10.07$ ,  $P < 0.01$ ; all Tukey *P*-values for length classes between 151–225 < 0.05; Fig. 7). Predicted *TS* was also significantly affected by orientation ( $F_{4,410} = 86.34$   $P < 0.01$ ; Fig. 7), with predicted *TS* being greater (2–3 dB re 1 m<sup>2</sup>) than measured *TS* for lateral (Tukey  $P < 0.01$ ) and oblique (Tukey  $P < 0.01$ ) orientations, but no significant difference existed for head/tail (Tukey  $P = 0.06$ ).

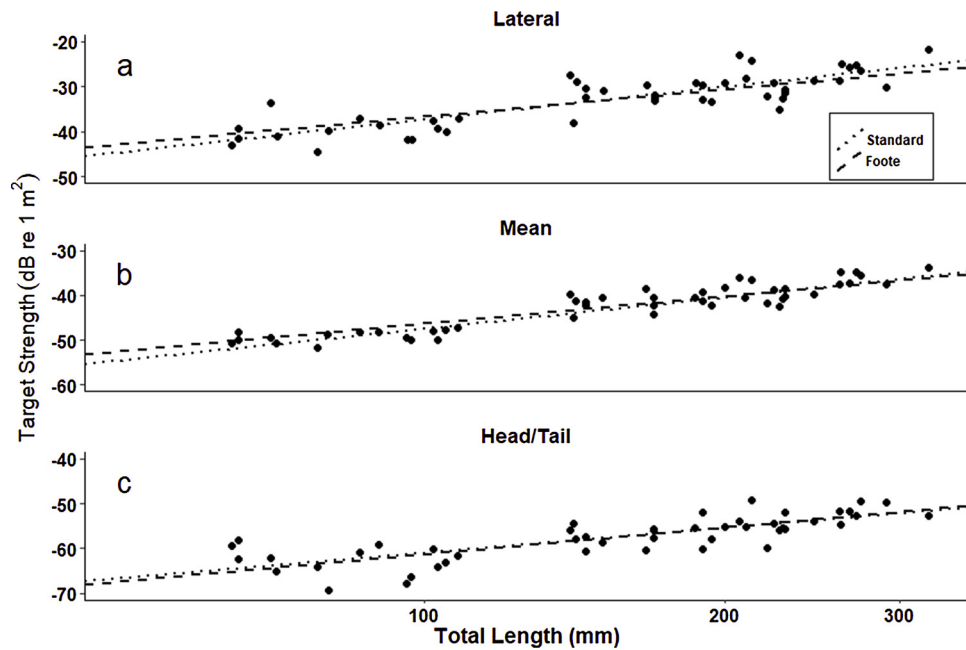


Fig. 5. Total length to target strength regressions for lateral aspect (a), average of all orientations (b) and head/tail aspect (c) fitting the a-coefficient (Standard) and fixing it at 20 (Foote, 1987b) for Gizzard Shad (n = 47, 64–321 mm, 3–223.8 g).

Table 4

Regression Coefficients for target strength equations ( $TS = a * \log_{10}(TL) + b$  for length,  $TS = a * \log_{10}(WT) + b$  for weight) derived from *ex situ* tank experiments with Gizzard Shad (*Dorosoma cepedianum*, n = 47, 64–321 mm, 3–223.8 g) at different orientations (Head-on fit data where fish were facing the transducer [90°], Lateral fit data where fish were perpendicular to the transducer [0° and 180°], and Mean fit data from all fish orientations (0 – 180° in 5° increments)).  $b_{20}$ -values are from models using a slope fixed at a = 20 (Foote, 1987b). P-value indicates whether slope was significantly different than 0. An asterisk denotes the parameter was statistically different between the two forms of the TS-TL equation.

Length						Weight		
	a	P-value	b	$b_{20}$	$r^2/r_{b20}^2$	a	b	$r^2$
Mean	23.02*	< 0.01	-93.53	-86.31	0.86/0.86	8.05	-54.74	0.85
Head-on	18.66	< 0.01	-98.42	-101.34	0.63/0.63	6.47	-67.37	0.63
Lateral	23.77	< 0.01	-84.83	-76.59	0.71/0.71	8.16	-45.17	

Table 5

Comparisons of model fits for 8 orientation-based and 2 non-orientation based models for Gizzard Shad data collected in tank experiments. Models ordered by AIC values.

Model Name	AIC	ΔAIC	d.f.	Weight
Catenary	9823.77	0	6	0.99
Poly <sub>2</sub>	9836.42	12.6	7	< 0.01
Trig <sub>sin</sub>	9873.99	50	6	< 0.01
Trig <sub>both</sub>	9875.44	51.4	7	< 0.01
ABV	10025.19	200.2	6	< 0.01
Kub <sup>3</sup>	10034.47	208.7	6	< 0.01
Kub <sup>5</sup>	10077.68	250.3	6	< 0.01
Kub	10129.7	304.1	6	< 0.01
Non-Orient	11203.47	1372.8	4	< 0.01
Foote	11297.56	1473.8	3	< 0.01

orientation.

3.3. Estimating uncertainty in biomass estimates caused by orientation changes

The hypothetical populations had different biomasses, though depending on their orientation, this was not always apparent from the biomass calculated using the TS-TL equations. The uniform population had the largest “true” biomass followed by the identical population biomass, but all populations had similar biomass estimates for

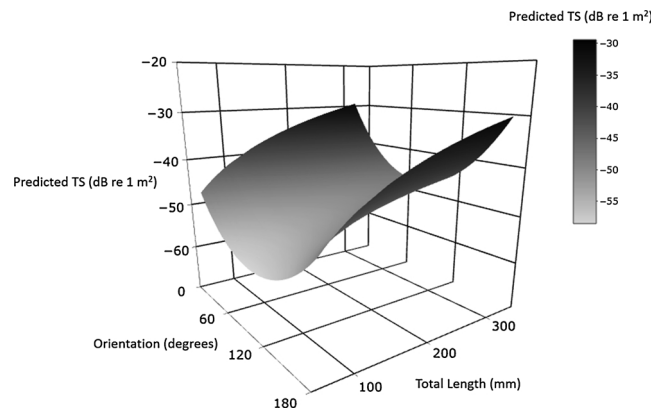


Fig. 6. Depiction of the change in target strength with changes in total length and orientation modelled using a catenary function derived from data collected with Gizzard Shad in tank trials. Darker color indicates stronger TS.

orientations greater than 40° from perpendicular (Fig. 8). Apparent biomass decreased exponentially as orientation increased from 0° to 90° (Fig. 8). Biomass is underestimated by approximately 60% in all populations with a 10° change in orientation and 80% with a 20° change in orientation (Fig. 8). Biomass can be underestimated by 90% if fish orientation deviates by 30° and over 95% when orientation is 75° from the expected value (Fig. 8).

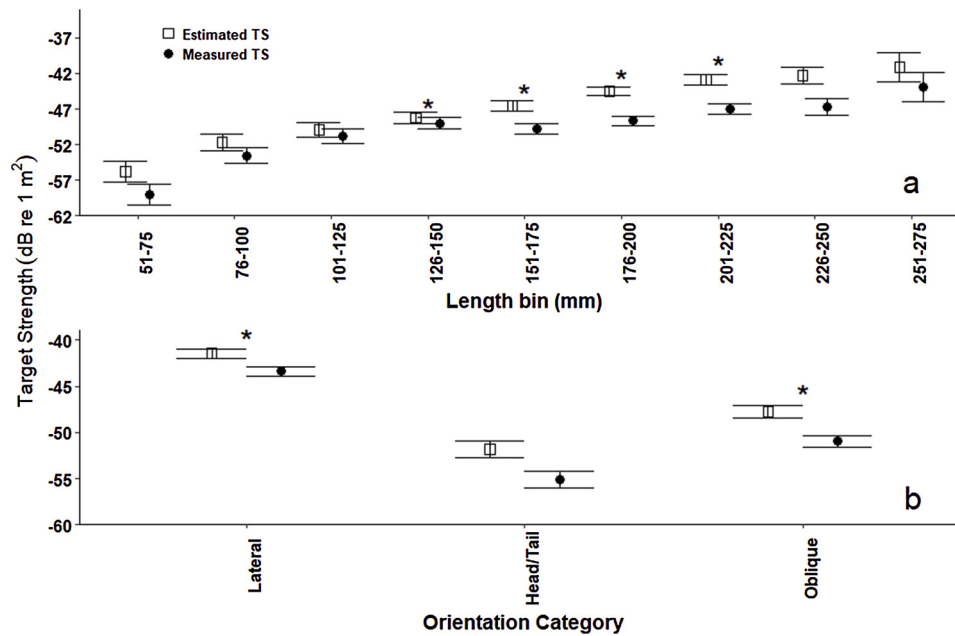


Fig. 7. Difference between measured target strength from a Simrad EK60 120 kHz transducer and predicted target strength derived from length (a) and orientation (b) data collected with an ARIS imaging SONAR using our catenary equation. Error bars represent 95% confidence intervals. Asterisks indicate significant differences.

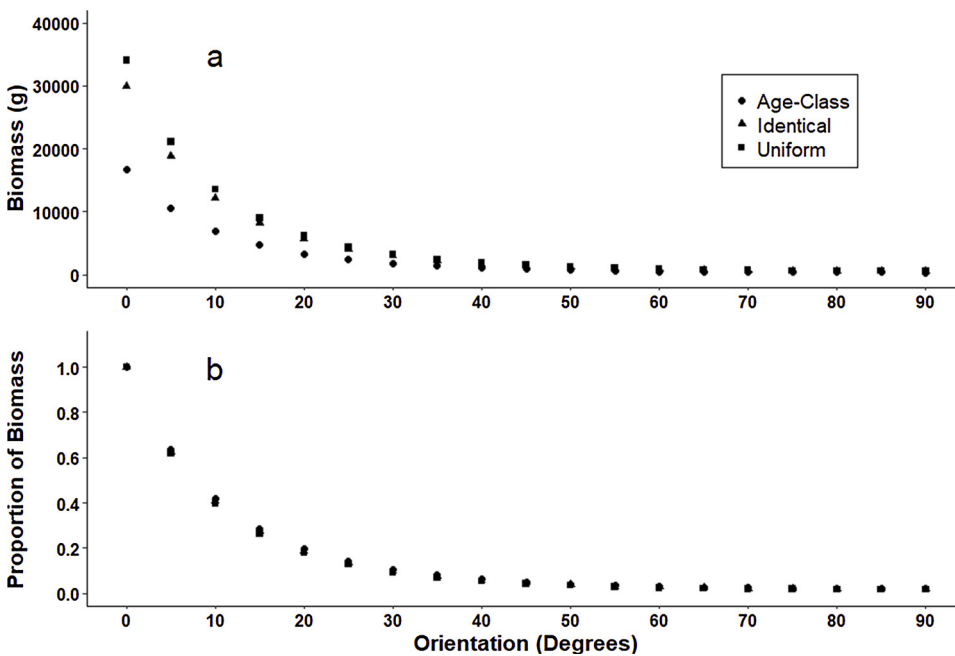


Fig. 8. Change in biomass (a) and proportion of “true” biomass (b) estimated for three simulated Gizzard Shad populations ( $n=1000$ ) when estimating total length of fish at different orientations with a TS-TL regression. First population contains all individuals 150 mm in length (Identical). Second consists of a random uniform distribution of fish 100–200 mm in length (Uniform). Third population has three age orientations with a TS-TL regression. First population contains all individuals 150 mm in length (Identical). Second consists of a random uniform distribution of fish 100–200 mm in length (Uniform). Third population has three age orientations with a TS-TL regression. Age-0 ( $n=700$ ) fish had a mean length of 100 mm ( $s.d. = 5$ ). Age-1 ( $n=250$ ) fish had a mean length of 150 mm ( $s.d. = 7.5$ ). Age-2 ( $n=50$ ) fish had a mean length of 190 mm ( $s.d. = 10$ ; Age Class).

### 3.4. Comparison of echo-integration results from different side-aspect TS-TL equations

Equation choice had a significant effect on density estimates from individually echo-integrated schools.  $Frou_{Pooled}$  had a significantly higher density estimate (mean density =  $1.1 \text{ fish m}^{-2}$ ) than all other equations ( $P < 0.01$ , Fig. 9).  $John_{All}$  ( $0.58 \text{ fish m}^{-2}$ ),  $John_{Foote}$  ( $0.54 \text{ fish m}^{-2}$ ) and  $Bos_{Pooled}$  ( $0.56 \text{ fish m}^{-2}$ ) had significantly greater density estimates than  $Bos_{Foote}$  ( $0.43 \text{ fish m}^{-2}$ ) and  $Kub_{All}$  ( $0.43 \text{ fish m}^{-2}$ ), but less than  $Frou_{Pooled}$  (Fig. 9). Density estimates using the  $Frou_{Pooled}$  equation were almost twice as large as any other equation (Fig. 9).

## 4. Discussion

We developed a side-aspect equation that predicts TS using TL and

fish orientation that could improve biomass estimates for Gizzard Shad from horizontal echosounders when fish orientation is known or can be measured. This equation generally performed well and provided much more realistic TS estimates of individual fish at different orientations than traditional horizontal equations that average TS across all orientations. This may not translate into significantly different fish biomass estimates in schools of fish that had random orientation because averaging TS would account for fish orientation, but could greatly improve biomass estimates in cases where the assumption of random orientation are not met (e.g., river fish, boat avoidance, migrating fish. etc; Draštk and Kubečka, 2005; Kubečka, 1994; Lilja et al., 2000).

One previous attempt to develop an orientation-specific TS-TL equation has been published (Kubečka, 1994). This study found a  $\cos^3$  function best described the effect of fish orientation on TS for a single size of fish (Kubečka, 1994). Lilja et al. (2000) added TL to Kubečka

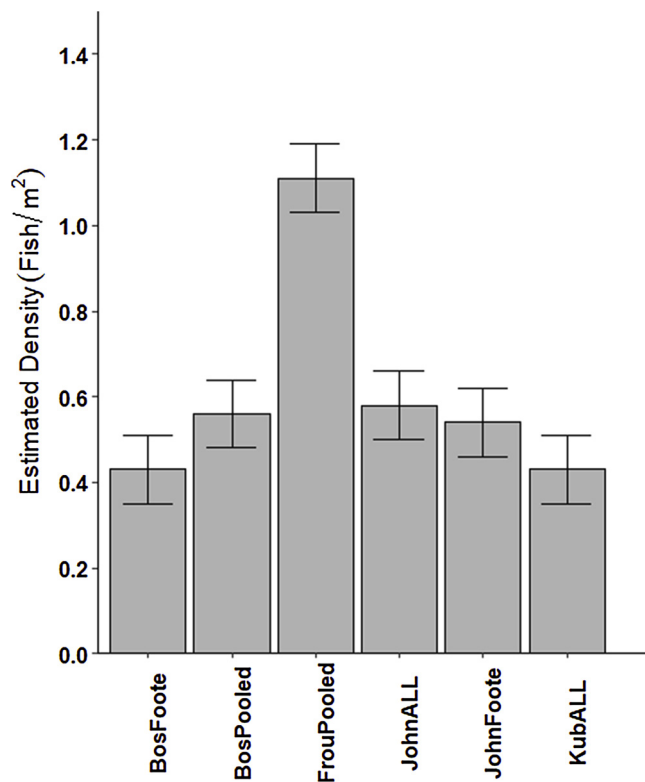


Fig. 9. Comparison of mean school density from 23 schools estimated using six different horizontal-aspect TS-TL equations. In addition to a non-orientation based mean TS-TL equations with random intercept (John<sub>ALL</sub>) and a variant with slope fixed at 20 (John<sub>Foote</sub>) from the current study, we tested Boswell and Wilson (2008) equations from pooled data for Gulf Menhaden (*Brevoortia patronus*) and Bay Anchovy (*Anchoa mitchilli*; Bos<sub>Pooled</sub>; Bos<sub>Foote</sub>), Frouzova's (2005) European pooled freshwater fish equation (Frou<sub>Pooled</sub>), and Kubečka's (1994) brown trout (*Salmo trutta*) model (Kub<sub>ALL</sub>).

(1994)'s aspect model to make it useful for echo integration and then calculated species-specific coefficients for Atlantic Salmon, Pike and Whitefish. We tested 8 different functions, including functions from Kubečka, 1994, and found a catenary function was considerably more parsimonious than all other functions for Gizzard Shad (Table 5; Kubečka, 1994; Lilja et al., 2000). Our new equation will provide more accurate Gizzard Shad TL estimates than non-orientation based equations when orientation information is available and is a function shape that should be considered in the development of species-specific horizontal-aspect TS-TL equations in the future.

When applying the catenary equation to live fish in the field as opposed to euthanized and tethered fish, the length and orientation of the ensonified individual affects accuracy of the size predicted from the measured TS (Fig. 7). There are several possible explanations for why accuracy varied with fish orientation and length class. First, the catenary equation may not be able to inflect as needed to match the observed TS using length and orientation information for all length-orientation combinations. However, we are unaware of any alternative equations that could be used and the catenary equation was the most parsimonious equation tested. Second, because the equation is being fit to a range of lengths and orientations, fit at some points may be sacrificed for lower residuals at other points. Third, there may have been additional variability introduced because length and orientation of free swimming fish were estimated using an imaging SONAR. Length estimates from imaging SONARs slightly underestimate fish length (Burwen et al., 2010) and are affected by target orientation (Tušer et al., 2014). Additionally, orientation measurements were difficult to acquire at some length-orientation combinations because small individuals disappear at head/tail orientations similar to observations by

Tušer et al., 2014. Therefore, ARIS® measurements from small (< 100 mm) individuals may have been inaccurate in some instances. Lastly, differences in transducer tilt (0° in lab and 3.5° downward in the net pen) could explain differences between predicted TS from the catenary equation and measured TS of live individuals because the tilt of targets could result in reduced TS (MacLennan et al., 1989; McQuinn and Winger, 2003).

The orientation-based equation can provide more accurate fish-size estimates, but requires knowledge of fish orientation, which can be acquired in multiple ways. First, orientation can be estimated by movements of a target on an x-z plane, tracked using a split-beam echosounder (Rodríguez-Sánchez et al., 2015). This approach does not estimate instantaneous orientation, but infers orientation based on linear movements of a target track over time (i.e., assumes fish are facing the direction they are moving; Rodríguez-Sánchez et al., 2015). This idea has also been implemented with a dual-beam echosounder and can estimate the slope of a moving fish (mm/ping) using the change in range on successive pings from a fixed transducer (Kubečka and Duncan, 1998b). Second, improvements in the application of Broad-band techniques have resulted in an ability to infer target orientation through increased range resolution and improved interpretation of scattering features of individual targets (Ito et al., 2015; Jaffe and Roberts, 2011; Lundgren and Nielsen, 2008; Stanton et al., 2010, 2003). A third approach, which was used when validating our orientation-based-equation, is pairing an imaging SONAR with a split-beam echosounder. Imaging SONARs can estimate orientation of individual fish that are solitary as well as fish at the edge of aggregations by calculating the range difference from head to tail of a target (Rose et al., 2005). Using imaging SONAR data, users can determine when fish within an aggregation are randomly or uniformly oriented. This allows the user to reduce the uncertainty associated with applying TS-TL regressions by applying an orientation-specific equation when it is needed. However, the range of imaging SONAR will restrict the use of this method to the first 15 m. These approaches can be implemented during hydroacoustic surveys to measure fish orientation for use in our orientation-based equation.

When orientation information is unavailable, a  $TS_{Mean}$ ,  $TS_{Lateral}$ , or  $TS_{Head/Tail}$  equation should be used, depending on whether orientation can be assumed. For example, when fish orientation can be assumed to be lateral (i.e. migratory movements within a river with transducer oriented perpendicular to river flow) or in the head-tail aspect (boat avoidance or other situation with fish moving toward or away from the transducer), the  $TS_{Lateral}$

$$10^{\left(\frac{TS+84.83}{23.77}\right)}$$

or  $TS_{Head/Tail}$

$$10^{\left(\frac{TS+101.34}{18.66}\right)}$$

equations, respectively, may produce appropriate fish sizes (Burwen and Fleischman, 1998; Draštk and Kubečka, 2005; Pedersen et al., 2009). This approach has been commonly used in riverine environments (Burwen and Fleischman, 1998; Thorne, 1998). Our orientation-based equation may also be suitable in these situations, but may not be as reliable because the curve fit compensated for all orientations whereas  $TS_{Lateral}$  and  $TS_{Head/Tail}$  equations were derived solely from lateral and head-on data. However, when orientation information is unavailable and orientation is assumed to be random,  $TS_{Mean}$  equations can be used to estimate biomass and density. Although the assumption of random orientation will be the least precise, it should be unbiased and result in accurate biomass estimates as long as there are equal numbers of individuals facing in all orientations. Therefore, our Gizzard Shad TS-TL equations could be applied in various sampling situations.

Based on the recommendations of Foote (1987b), we derived two forms of each TS-TL equation ( $TS_{Mean}$ ,  $TS_{Lateral}$  and  $TS_{Head/Tail}$ ), a standard model with fitted slope, and a Foote (1987b) variant with a

slope fixed at 20 (to facilitate comparison among equations for different species). Our  $TS_{\text{Lateral}}$  and  $TS_{\text{Head/Tail}}$  equations performed similarly with and without the fixed slope and either equation would therefore be acceptable to use (Table 4). Only the  $TS_{\text{Mean}}$  equation produced significantly different results between the standard ( $a = 23.02, b = -93.53$ ) and Foot (1987b) variants ( $a = 20, b = -86.31$ ; Table 4). In this case, the standard ( $a$  is fitted) equation should be used to better describe the relationship between Gizzard Shad size and  $TS$ .

Our results suggest using incorrect orientation information can lead to biased fish size estimations resulting in incorrect biomass estimates (Fig. 8). These results are similar to Boswell et al. (2009), but our results suggest that errors occur at a greater initial rate (60% underestimated at  $\theta = 10^\circ$ ) as fish orientation changes with Gizzard Shad relative to Gulf Menhaden (50% underestimated at  $\theta = 10^\circ$ ; Fig. 8). This can be explained by the difference in orientation-based equations. Boswell et al., 2009 uses a parabolic curve to describe the change in  $TS$  while we use an equation with a hyperbolic cosine function (Table 2). The hyperbolic cosine function allows our equation to have a greater initial decrease while flattening at the bottom instead of the continuous decrease of the parabolic function. Our results reinforce the need for orientation data while collecting data with a horizontally-oriented echosounder given the extreme (underestimate by up to 95%) differences in biomass estimates when orientation is not incorporated in length calculations (Fig. 8). The use of incorrect Gizzard Shad biomass estimates may lead to many management issues including poor growth rate and survival of stocked fish if biomass is overestimated (Byström et al., 1998; Kolar et al., 2003; Olson et al., 1995).

Many equations have been proposed to predict average  $TS$  for individual species (Gulf Menhaden Boswell et al., 2009, Rainbow Smelt *Osmorus mordax* Brooking and Rudstam (2009), skipjack tuna *Katsuwonus pelamis* Boyra et al., 2018 and Antarctic Krill Chu et al. 1993 among others) or groups of species (salmonids Dahl and Mathisen 1983, Gulf Menhaden and Anchovy Boswell and Wilson, 2008, Brown Trout, Perch *Perca fluviatilis*, Bream *Abramis brama*, Roach, Carp *Cyprinus carpio* and Bleak *Alburnus alburnus* Frouzova et al., 2005 and Rainbow Smelt, Bloaters *Coregonus hovi*, and Alewife *Alosa pseudoharengus* Fleischer et al., 1997), but only limited comparisons have been made between these equations (Boswell et al., 2008; Frouzova et al., 2005; Godlewska et al., 2012). We found that the  $TS$ - $TL$  equation used when echo integrating can have a significant effect on density estimates (Fig. 9). Applying the  $Frou_{\text{pooled}}$  ( $1.11 \text{ fish m}^{-2}$ ) equation in our scenario doubled density estimates from the Gizzard Shad specific standard ( $0.58 \text{ fish m}^{-2}$ ) and Foote (1987b) variants ( $0.54 \text{ fish m}^{-2}$ )  $TS$ - $TL$  equations (Fig. 9). Overestimating Gizzard Shad biomass could cause erroneously high stocking rates of piscivorous predators. Therefore, it is beneficial to derive species-specific  $TS$ - $TL$  equations to ensure proper  $TS$ - $TL$  conversions are applied to hydroacoustic data, especially when data are used for making management decisions.

There are many other factors that can influence measured  $TS$  besides orientation in the  $x$ - $z$  plane and  $TL$  (e.g., changes in swim bladder sound reflectance) that should be considered (Foote, 1980; Kubečka, 1994; Ona, 1990). Fish behavior, such as vertical migrations (Harden-Jones et al., 1981; Knudsen and Gjelland, 2004; Vabø et al., 2002) and boat avoidance behaviors (Draštík and Kubečka, 2005; Vabø et al., 2002), can affect measured  $TS$  by changing fish tilt and roll (Love, 1977; McQuinn and Winger, 2003; Nakken and Olsen, 1977). These factors influence  $TS$  of individual fish, but when averaged over an entire survey, these errors are likely minimized (Fedotova and Shatoba, 1983; MacLennan et al., 1989). Fish physiology such as fat content, gonadal maturity, method of airbladder inflation (i.e. physostome vs physoclist), ontogeny, and stomach content can also affect measured  $TS$  (Foote, 1987b; Horne, 2003; Ona, 1990; Ona et al., 2001). Therefore, fish of similar size and orientation can have different measured  $TS$ 's and these potential sources of variability need to be considered when applying  $TS$ - $TL$  relationships.

Derivation of orientation-based side-aspect  $TS$ - $TL$  equations can

provide increased accuracy of biomass estimates from horizontally-oriented hydroacoustic surveys when orientation information is available. Our non-orientation based equations can also be used as a more accurate equation for Gizzard Shad in various situations when orientation information is not available (Fig. 9). Species-specific  $TS$ - $TL$  equations should be used when available to ensure estimates are reliable. When species-specific equations are not available, caution should be taken when selecting  $TS$ - $TL$  equations because equation choice can have a significant effect on abundance estimates. We recommend the use of species-specific, orientation-based equations when possible, but non-orientation equations can also be useful in some circumstances.

## Acknowledgements

Funding: This work was supported by Federal Aid in Sportfish Restoration Project F-94-R, administered by the Oklahoma Department of Wildlife Conservation; the USDA National Institute of Food and Agriculture Hatch project no 1,006,561; and the Division of Agricultural Sciences and Natural Resources at Oklahoma State University. We also thank Alexis Whiles and Blake Crispin for help with data collection. This is contribution #139 from the Center for Coastal Oceans Research in the Institute of Water and Environment at Florida International University.

## References

- Balk, H., Søvegiarto, B.S., Tušer, M., Frouzová, J., Muška, M., Draštík, V., Baran, R., Kubečka, J., 2017. Surface-induced errors in target strength and position estimates during horizontal acoustic surveys. *Fish. Res.* 188, 149–156.
- Boswell, K.M., Kaller, M.D., Cowan Jr, J.H., Wilson, C.A., 2008. Evaluation of target strength-fish length equation choices for estimating estuarine fish biomass. *Hydrobiologia* 610, 113–123.
- Boswell, K.M., Roth, B.M., Cowan Jr, J.H., 2009. Simulating the effects of side-aspect fish orientation on acoustic biomass estimates. *ICES J. Mar. Sci.* 66, 1398–1403.
- Boswell, K.M., Wilson, C.A., 2008. Side-aspect target-strength measurements of bay anchovy (*Anchoa mitchilli*) and Gulf menhaden (*Brevoortia patronus*) derived from ex situ experiments. *ICES J. Mar. Sci.* 65, 1012–1020.
- Boswell, K.M., Wilson, M.P., Wilson, C.A., 2007. Hydroacoustics as a tool for assessing fish biomass and size distribution associated with discrete shallow water estuarine habitats in Louisiana. *Estuaries Coasts* 30, 607–617.
- Boyra, G., Moreno, G., Sobradillo, B., Pérez-Arjona, I., Sancristobal, I., Demer, D.A., Ratilal, H.P., 2018. Target strength of skipjack tuna (*Katsuwonus pelamis*) associated with fish aggregating devices (FADs). *ICES J. Mar. Sci.* 75, 1790–1802.
- Burwen, D.L., Fleischman, S.J., 1998. Evaluation of side-aspect target strength and pulse width as potential hydroacoustic discriminators of fish species in rivers. *Can. J. Fish. Aquat. Sci.* 55, 2492–2502.
- Brooking, T.E., Rudstam, L.G., 2009. Hydroacoustic target strength distributions of alewives in a net-cage compared with field surveys: deciphering target strength distributions and effect on density estimates. *Transactions of the American Fisheries Society*. 138, 471–486.
- Burwen, D.L., Fleischman, S.J., Miller, J.D., 2010. Accuracy and precision of salmon length estimates taken from DIDSON sonar images. *Trans. Am. Fish. Soc.* 139, 1306–1314.
- Byström, P., Persson, L., Wahlström, E., 1998. Competing predators and prey: juvenile bottlenecks in whole-lake experiments. *Ecology* 79, 2153–2167.
- Carline, R.F., Johnson, B.L., Hall, T.J., 1984. Estimation and interpretation of proportional stock density for fish populations in Ohio impoundments. *N. Am. J. Fish. Manag.* 4, 139–154.
- Dahl, P., Mathisen, O., 1983. Measurement of fish target strength and associated directivity at high frequencies. *The Journal of the Acoustical Society of America*. 73, 1205–1211.
- Djemali, I., Guillard, J., Yule, D.L., 2017. Seasonal and diel effects on acoustic fish biomass estimates: application to a shallow reservoir with untargeted common carp (*Cyprinus carpio*). *Mar. Freshw. Res.* 68, 528–537.
- Draštík, V., Kubečka, J., 2005. Fish avoidance of acoustic survey boat in shallow waters. *Fish. Res.* 72, 219–228.
- Evans, N., Shoup, D., Glover, D., 2014. A simplified approach for estimating age-0 gizzard shad prey supply and predator demand. *Fish. Manag. Ecol.* 21, 140–154.
- Fedotova, T., Shatoba, O., 1983. Acoustic Backscattering Cross Section of Cod Averaged by Sizes and Inclination of Fish. *FAO Fisheries Report (FAO)*.
- Fleischer, G.W., Argyle, R.L., Curtis, G.L., 1997. In situ relations of target strength to fish size for Great Lakes pelagic planktivores. *Trans. Am. Fish. Soc.* 126, 786–794.
- Foote, K.G., 1980. Importance of the swimbladder in acoustic scattering by fish: a comparison of gadoid and mackerel target strengths. *J. Acoust. Soc. Am.* 67, 2084–2089.
- Foote, K.G., 1987a. Calibration of acoustic instruments for density estimation: a practical guide. *Int. Council Explor. Sea Coop. Res. Rep.* 144, 57p.
- Foote, K.G., 1987b. Fish target strengths for use in echo integrator surveys. *J. Acoust. Soc. Am.* 82, 981–987.

- Foote, K.G., Aglen, A., Nakken, O., 1986. Measurement of fish target strength with a split-beam echo sounder. *J. Acoust. Soc. Am.* 80, 612–621.
- Frouzova, J., Kubečka, J., Balk, H., Frouz, J., 2005. Target strength of some European fish species and its dependence on fish body parameters. *Fish. Res.* 75, 86–96.
- Gastauer, S., Scoulding, B., Parsons, M., 2017. Estimates of variability of goldband snapper target strength and biomass in three fishing regions within the Northern Demersal Scalefish Fishery (Western Australia). *Fish. Res.* 193, 250–262.
- Godlewski, M., Frouzova, J., Kubečka, J., Wiśniewolski, W., Szlakowski, J., 2012. Comparison of hydroacoustic estimates with fish census in shallow Malta Reservoir—which TS/L regression to use in horizontal beam applications? *Fish. Res.* 123, 90–97.
- Gorska, N., Ona, E., 2003. Modelling the acoustic effect of swimbladder compression in herring. *ICES J. Mar. Sci.* 60, 548–554.
- Harden-Jones, F., Scholes, P., Suomala, J., 1981. The swimbladder, vertical movements, and the target strength of fish. Meeting on Hydroacoustical Methods For The Estimation Of Marine Fish Populations. The Charles Stark Draper Laboratory, Inc, Cambridge, MA, USA.
- Horne, J.K., 2003. The influence of ontogeny, physiology, and behaviour on the target strength of walleye pollock (*Theragra chalcogramma*). *ICES J. Mar. Sci.* 60, 1063–1074.
- Ito, M., Matsuo, I., Imaizumi, T., Akamatsu, T., Wang, Y., Nishimori, Y., 2015. Target strength spectra of tracked individual fish in schools. *Fish. Sci.* 81, 621–633.
- Jaffe, J.S., Roberts, P.L., 2011. Estimating fish orientation from broadband, limited-angle, multiview, acoustic reflections. *J. Acoust. Soc. Am.* 129, 670–680.
- Jester, D., Jensen, B., 1972. Life history and ecology of the gizzard shad, *Dorosoma cepedianum* (Le Sueur), with reference to Elephant Butte Lake New Mexico State University. Agriculture Experiment Station. Research Report, Las Cruces.
- Johnson, B.M., Stein, R.A., Carline, R.F., 1988. Use of a quadrat rotenone technique and bioenergetics modeling to evaluate prey availability to stocked piscivores. *Trans. Am. Fish. Soc.* 117, 127–141.
- Johnson, G.R., Shoup, D.E., Boswell, K.M., 2019. Accuracy and precision of hydroacoustic estimates of Gizzard Shad abundance using horizontal beaming. *Fish. Res.* 212, 81–86.
- Knudsen, F.R., Gjelland, K.Ø., 2004. Hydroacoustic observations indicating swimbladder volume compensation during the diel vertical migration in coregonids (*Coregonus lavaretus* and *Coregonus albula*). *Fish. Res.* 66, 337–341.
- Knudsen, F.R., Særgrov, H., 2002. Benefits from horizontal beaming during acoustic survey: application to three Norwegian lakes. *Fish. Res.* 56, 205–211.
- Kolar, C.S., Wahl, D.H., Hooe, M.L., 2003. Piscivory in juvenile walleyes: relative importance of prey species, timing of spawning of prey fish, and density on growth and survival. *Trans. Am. Fish. Soc.* 132, 679–690.
- Kubečka, J., 1994. Simple model on the relationship between fish acoustical target strength and aspect for high-frequency sonar in shallow waters. *J. Appl. Ichthyol.* 10, 75–81.
- Kubečka, J., Duncan, A., 1998a. Acoustic size vs. Real size relationships for common species of riverine fish. *Fish. Res.* 35, 115–125.
- Kubečka, J., Duncan, A., 1998b. Diurnal changes of fish behaviour in a lowland river monitored by a dual-beam echosounder. *Fish. Res.* 35, 55–63.
- Kubečka, J., Frouzová, J., Balk, H., Čech, M., Draščík, V., Prchalová, M., 2009. Regressions for conversion between target strength and fish length in horizontal acoustic surveys. In: Papadakis, J.S., Bjorno, L. (Eds.), *Underwater Acoustic Measurements, Technologies & Results*, pp. 1039–1044.
- Kubečka, J., Wittingerova, M., 1998. Horizontal beaming as a crucial component of acoustic fish stock assessment in freshwater reservoirs. *Fish. Res.* 35, 99–106.
- Kuznetsova, A., Brockhoff, P.B., Christensen, R.H.B., 2017. {lmerTest} package: tests in linear mixed effects models. *J. Stat. Softw.*
- Lavery, A.C., Bassett, C., Lawson, G.L., Jech, J.M., Demer, He.D., 2017. Exploiting signal processing approaches for broadband echosounders. *ICES J. Mar. Sci.* 74, 2262–2275.
- Lee, W.-J., Stanton, T.K., 2016. Statistics of broadband echoes: application to acoustic estimates of numerical density of fish. *IEEE J. Ocean. Eng.* 41, 709–723.
- Lian, Y., Huang, G., Godlewski, M., Cai, X., Li, C., Ye, S., Liu, J., Li, Z., 2017. Hydroacoustic estimates of fish biomass and spatial distributions in shallow lakes. *Chinese J. Oceanol. Limnol.* 1–11.
- Lilja, J., 2004. Assessment of Fish Migration in Rivers by Horizontal Echo Sounding: Problems Concerning Side-aspect Target Strength. University of Jyväskylä.
- Lilja, J., Marjomäki, T.J., Riikonen, R., Jurvelius, J., 2000. Side-aspect target strength of Atlantic salmon (*Salmo salar*), brown trout (*Salmo trutta*), whitefish (*Coregonus lavaretus*), and pike (*Esox lucius*). *Aquat. Living Resour.* 13, 355–360.
- Love, R.H., 1977. Target strength of an individual fish at any aspect. *J. Acoust. Soc. Am.* 62, 1397–1403.
- Lundgren, B., Nielsen, J.R., 2008. A method for the possible species discrimination of juvenile gadoids by broad-bandwidth backscattering spectra vs. Angle of incidence. *ICES J. Mar. Sci.* 65, 581–593.
- MacLennan, D., Hollingworth, C., Armstrong, F., 1989. Target strength and the tilt angle distribution of caged fish. *Proc. Inst. Acoust.* 11, 11–20.
- MacLennan, D., Simmonds, E.J., 2013. *Fisheries Acoustics*. Springer Science & Business Media.
- McClatchie, S., Macaulay, G., Hanchet, S., Coombs, R.F., 1998. Target strength of southern blue whiting (*Micromesistius australis*) using swimbladder modelling, split beam and deconvolution. *ICES J. Mar. Sci.* 55, 482–493.
- McQuinn, I.H., Winger, P.D., 2003. Tilt angle and target strength: target tracking of Atlantic cod (*Gadus morhua*) during trawling. *ICES J. Mar. Sci.* 60, 575–583.
- Michaletz, P.H., 1997. Influence of abundance and size of age-0 gizzard shad on predator diets, diet overlap, and growth. *Trans. Am. Fish. Soc.* 126, 101–111.
- Michaletz, P.H., 1998. Effects on sport fish growth of spatial and temporal variation in age-0 gizzard shad availability. *N. Am. J. Fish. Manag.* 18, 616–624.
- Miranda, L.E., 1983. Average ichthyomass in Texas large impoundments. *Proc. Texas Chapter Am. Fish. Soc.* 6, 58–67.
- Nakken, O., Olsen, K., 1977. Target strength measurements of fish. *ICES*.
- Nielsen, J.R., Lundgren, B., 1999. Hydroacoustic ex situ target strength measurements on juvenile cod (*Gadus morhua* L.). *ICES J. Mar. Sci.* 56, 627–639.
- Olson, M.H., Mittelbach, G., Osenberg, C., 1995. Competition between predator and prey: resource-based mechanisms and implications for stage-structured dynamics. *Ecology* 76, 1758–1771.
- Ona, E., 1990. Physiological factors causing natural variations in acoustic target strength of fish. *J. Mar. Biol. Assoc. U.K.* 70, 107–127.
- Ona, E., Zhao, X., Svellingen, I., Fosseidengen, J., 2001. Seasonal variation in herring target strength. Herring: expectations for a New Millennium. 461, 461–487.
- Parker-Stetter, S.L., Rudstam, L.G., Sullivan, P., Warner, D., 2009. Standard Operating Procedures for Fisheries Acoustic Surveys in the Great Lakes.
- Pedersen, B., Trevorrow, M.V., 1999. Continuous monitoring of fish in a shallow channel using a fixed horizontal sonar. *J. Acoust. Soc. Am.* 105, 3126–3135.
- Pedersen, G., Handegard, N.O., Ona, E., 2009. Lateral-aspect, target-strength measurements of in situ herring (*Clupea harengus*). *ICES Mar. Sci.: J. du Conseil.* 66, 1191–1196.
- Peña, H., Foote, K.G., 2008. Modelling the target strength of *Trachurus symmetricus murphyi* based on high-resolution swimbladder morphometry using an MRI scanner. *ICES J. Mar. Sci.* 65, 1751–1761.
- Pinheiro, J., Bates, D., DebRoy, S., 2017. *nlme: Linear and Nonlinear Mixed Effects Models*. R Core Team.
- Pollom, R.A., Rose, G.A., 2015. Size-based hydroacoustic measures of within-season fish abundance in a boreal freshwater ecosystem. *PLoS One* 10, e0124799.
- Roberts, J.J., Höök, T.O., Ludsins, S.A., Pothoven, S.A., Vanderploeg, H.A., Brandt, S.B., 2009. Effects of hypolimnetic hypoxia on foraging and distributions of Lake Erie yellow perch. *J. Exp. Mar. Biol. Ecol.* 381, S132–S142.
- Rodríguez-Sánchez, V., Encina-Encina, L., Rodríguez-Ruiz, A., Sánchez-Carmona, R., 2015. Horizontal target strength of *Luciobarbus* sp. in ex situ experiments: Testing differences by aspect angle, pulse length and beam position. *Fish. Res.* 164, 214–222.
- Rodríguez-Sánchez, V., Encina-Encina, L., Rodríguez-Ruiz, A., Sánchez-Carmona, R., 2016. Do choice range measurements affect the target strength (TS) of fish in horizontal beaming hydroacoustics? *Fish. Res.* 173, 4–10.
- Rose, C.S., Stoner, A.W., Matteson, K., 2005. Use of high-frequency imaging sonar to observe fish behaviour near baited fishing gears. *Fish. Res.* 76, 291–304.
- SAS Proc Glimmix; SAS Institute Inc, 2017. *SAS/STAT® 14.3 User's Guide*. SAS Institute Inc, Cary, NC.
- Schael, D.M., Rice, J.A., Degan, D.J., 1995. Spatial and temporal distribution of threadfin shad in a southeastern reservoir. *Trans. Am. Fish. Soc.* 124, 804–812.
- Schramm, H.L., Kraai, J.E., Munger, C.R., 1999. Intensive stocking of striped bass to restructure a gizzard shad population in a eutrophic Texas reservoir. Proceedings of the Annual Conference Southeastern Association of Fish and Wildlife Agencies.
- Scoulding, B., Gastauer, S., MacLennan, D.N., Fässler, S.M., Copland, P., Fernandes, P.G., 2017. Effects of variable mean target strength on estimates of abundance: the case of Atlantic mackerel (*Scomber scombrus*). *ICES J. Mar. Sci.* 74, 822–831.
- Simmonds, J., MacLennan, D.N., 2005. *Fisheries Acoustics: Theory and Practice*. John Wiley & Sons.
- Stanton, T.K., Chu, D., Jech, J.M., Irish, J.D., 2010. New broadband methods for resonance classification and high-resolution imagery of fish with swimbladders using a modified commercial broadband echosounder. *ICES J. Mar. Sci.* 67, 365–378.
- Stanton, T.K., Reeder, D.B., Jech, J.M., 2003. Inferring fish orientation from broadband-acoustic echoes. *ICES J. Mar. Sci.* 60, 524–531.
- Storck, T.W., 1986. Importance of gizzard shad in the diet of largemouth bass in Lake Shelbyville, Illinois. *Trans. Am. Fish. Soc.* 115, 21–27.
- Thomas, G., Kirsch, J., Thorne, R.E., 2002. Ex situ target strength measurements of Pacific herring and Pacific sand lance. *N. Am. J. Fish. Manag.* 22, 1136–1145.
- Thorne, R.E., 1998. Review: experiences with shallow water acoustics. *Fish. Res.* 35, 137–141.
- Trevorrow, M.V., 1998. Boundary scattering limitations to fish detection in shallow waters. *Fish. Res.* 35, 127–135.
- Tušer, M., Frouzová, J., Balk, H., Muška, M., Mrkvička, T., Kubečka, J., 2014. Evaluation of potential bias in observing fish with a DIDSON acoustic camera. *Fish. Res.* 155, 114–121.
- Urick, R.J., Hoover, R.M., 1956. Backscattering of sound from the sea surface: its measurement, causes, and application to the prediction of reverberation levels. *J. Acoust. Soc. Am.* 28, 1038–1042.
- Vabø, R., Olsen, K., Huse, I., 2002. The effect of vessel avoidance of wintering Norwegian spring spawning herring. *Fish. Res.* 58, 59–77.
- Van Den Avyle, M.J., Boxrucker, J., Michaletz, P., Vondracek, B., Ploskey, G.R., 1995a. Comparison of catch rate, length distribution, and precision of six gears used to sample reservoir shad populations. *N. Am. J. Fish. Manag.* 15, 940–955.
- Van Den Avyle, M.J., Ploskey, G.R., Bettoli, P.W., 1995b. Evaluation of gill-net sampling for estimating abundance and length frequency of reservoir shad populations. *N. Am. J. Fish. Manag.* 15, 898–917.
- Warner, D.M., Rudstam, L.G., Klumb, R.A., 2002. In situ target strength of alewives in freshwater. *Trans. Am. Fish. Soc.* 131, 212–223.
- Weih, D., 1973. *Hydromechanics of Fish Schooling*. pp. 290.
- Wilde, G.R., 1995. Gill net sample size requirements for temperate basses, shads, and catfishes. Proceedings of the Annual Conference Southeastern Association of Fish and Wildlife Agencies.
- Yule, D.L., 2000. Comparison of horizontal acoustic and purse-seine estimates of salmonid densities and sizes in eleven Wyoming waters. *N. Am. J. Fish. Manag.* 20, 759–775.